The Korean Journal of Ceramics, 7[2] 85-92 (2001)

Microstructural, Electrical and Optical Features of ZnO Thin Films Prepared by RF Sputter Techniques

Jung Ho Choi, Byung Jin Kim and Nam Hee Cho†

Department of Materials Science and Engineering, Inha University, Inchon 402-751, Korea

(Received May 31, 2000 · Accepted June 13, 2001)

Thin films of ZnO and Al doped ZnO were prepared by rf magnetron sputter techniques. When the oxygen fraction in Ar-O_2 sputter gas was about 2.0%, the films exhibited the composition of Zn:O=1.05:1. The films prepared at 250 W contain larger grains than the films grown at 100 W. However, high deposition rate seems to deteriorates the crystallinity as well as Al-substitution, resulting in lower concentration of mobile electrons. The Al-doped ZnO films which were deposited at 500°C show resistance of 1×10^{-2} Wcm; optical band gap of the films ranges from 3.25 to 3.40 eV. These electrical and optical features are related with microstructural as well as crystalline characteristics of the films.

Key words: ZnO, Al-doped ZnO, Thin film, Sputter, Sputter gas, Microstructure

I. Introduction

ZnO has attracted much attention over the last decade due to its desirable and unique characteristics like semiconducting behavior, optical transparency, piezoelectricity, etc. Thin films of ZnO with the physical characteristics have become more needed in microcircuit systems, as electrical devices have tended to become smaller and lighter recently.

The ZnO films can be used as transparent electrode due to the high optical transparency and electrical conductivity when the films are doped with particular elements in III or IV periods.[1-3] Moreover these films have higher chemical stability in hydrogen plasma compared with other transparent conducting films such as indium tin oxide (ITO), F- or Sb-doped SnO. The films can also be used to determine the micro-concentration of oxygen or trimethylamine (TMA) present in odour by using the varied electrical conductivity vs. chemisorption of oxygen gas.[4-6] Because the ZnO films are very sensitive to various gases and have a high response speed without consuming the gas, the films are expected to be increasingly developed for various sensors; for such applications the microstructural features and physical properties of the films should be controlled by adjusting thin film growing parameters.

Various thin film growing techniques such as the physical vapor deposition (PVD) and the chemical vapor deposition (CVD) are applicable to deposit ZnO thin films. Among them the rf magnetron sputter deposition technique has merits of simplicity of equipment and fast depositiion rate, and also has several deposition parameters which can be controlled. These parameters include sputter gas, working pressure, substrate temperature, substrate-target geometry and sputter power. As ways of controlling the microstructural features and physical properties of the films, impurity doping, post-deposition heat-treatment and post-deposition surface-treatment have also been performed. These deposition parameters and post-deposition treatments have con-

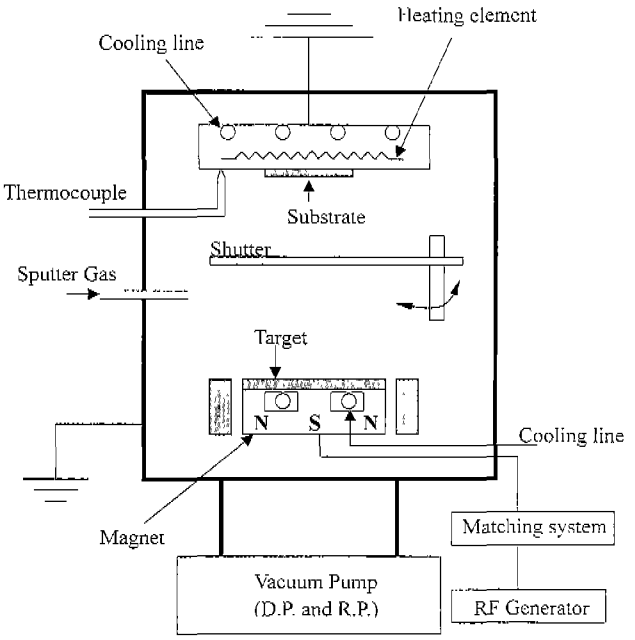

Fig. 1. Schematic diagram of the rf magnetron sputter system.

†Corresponding author: nhcho@inha.ac.kr

siderable influence on the surface morphology and microstructure of the films which are directly relatded to the physical and chemical properties.

However, only a small number of research papers have been reported on the microstructure of the ZnO polycrystalline films prepared by rf magnetron sputter, partly because of the restrictions caused by small grain size and random geometric relation among the grains.[7,8] As a result, the microstructural features, especially grain boundary structure and misorientation relations among the grains in the thin films have not been revealed well enough.

In this study, we investigated the relationships of surface morphology, microstructure, chemical composition and physical characteristics of ZnO thin films with film preparation parameters such as sputter gas, substrate temperature and sputter power. In particular, the effect of post-deposition surface-sputter as well as Al addition in the films on the microstructural characteristics, electrical and optical properties were investigated in detail.

II. Experimental

Thin films of ZnO and Al-doped ZnO (AZO) were prepared by rf magnetron sputter techniques. A schematic illustration of the sputter system used in this experiment is shown in Fig. 1. The distance between the substrate and the target is about 4.5 cm. Hot pressed pure ZnO (99.99%) ceramics and ZnO ceramics doped with 2 at.% Al_2O_3 were used as targets for ZnO and AZO films, respectively. Sputter gas consisted of a mixture of Ar-O_2. The fraction (R) of oxygen in

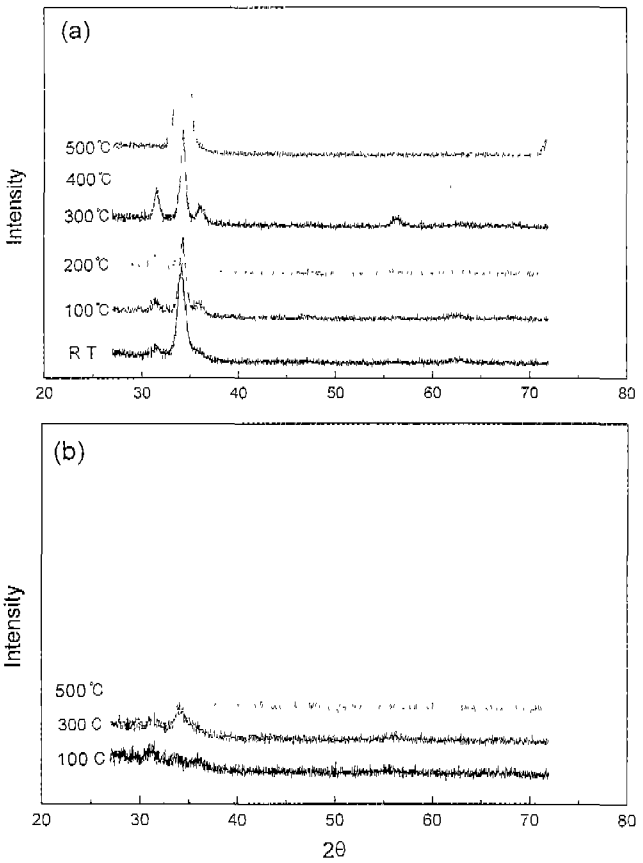

Fig. 2. XRD patterns of (a) the ZnO and (b) Al doped ZnO films. The films were prepared in sputter gas of R=1.3% at 250 W. The substrate temperature ranged from R.T. to 500℃.

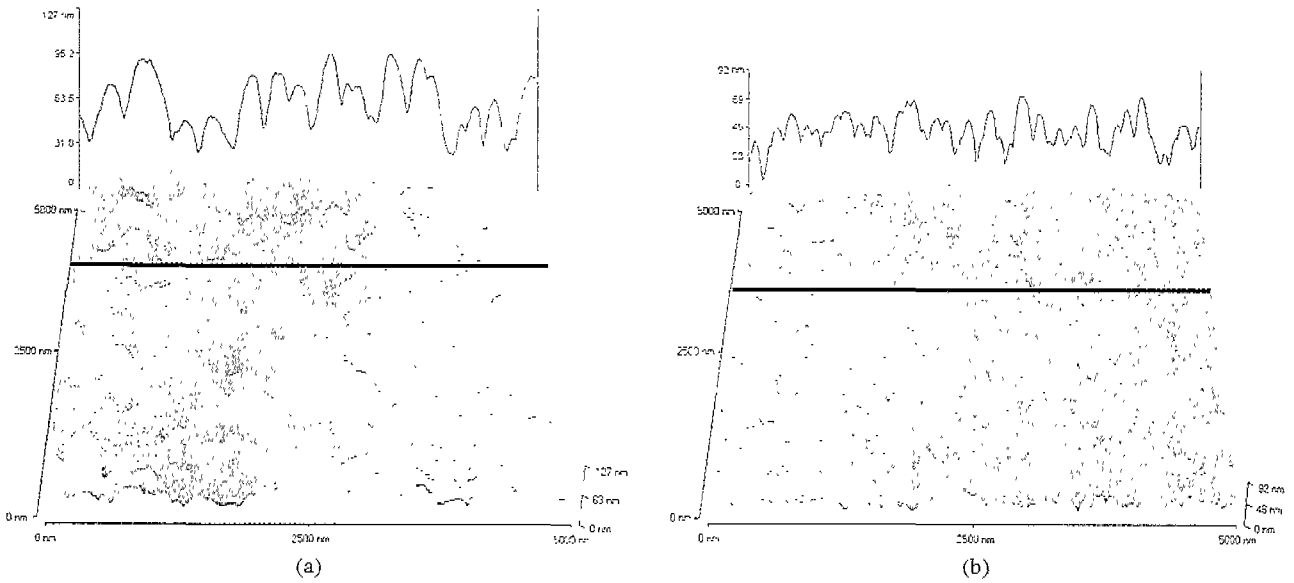

	(a)	(b)
Roughness (Ra, nm)	14.39	10.09
Grain Size (nm)	200~500	90~250

Fig. 3. AFM images of (a) the ZnO and (b) the AZO films. The films were deposited in pure Ar gas at 150 W; the substrate temperature was 300℃.

the sputter gas in this paper is the ratio of oxygen to argon gas inserted into the reaction chamber. It is expressed by following equation (1). Details of the deposition conditions are summarized in Table 1.

$$R\% = O_2/Ar \times 100 \quad (1)$$

The thickness of the films was measured using a surface profiler (alpha-step 500). The Van der Pauw method was employed to measure the electrical resistivity and Hall mobility of the films. The optical transmittance in the visible range was measured using a UV-visible spectrometer (UV-2401). The surface morphology and roughness of the

Table 1. Deposition Condition of the ZnO Thin Films

Deposition parameter	Experimental range
Target(2"1/6")	ZnO, Al:ZnO
Substrate	slide glass
Sputter power (watt)	50-250 (rf)
Sputter gas	Ar, Ar-O_2 (O_2/Ar=0-50%)
Background pressure (Torr)	10^{-6}
Working pressure (Torr)	10^{-3}
Substrate temperature (°C)	R.T.-500

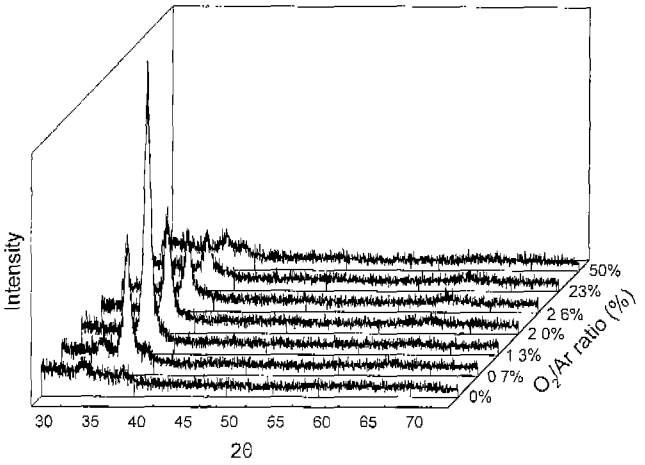

Fig. 4. XRD patterns of the ZnO films. The films were prepared at R.T. for 1 hr; the R value ranged from 0 to 50%; the sputter power was 250 W.

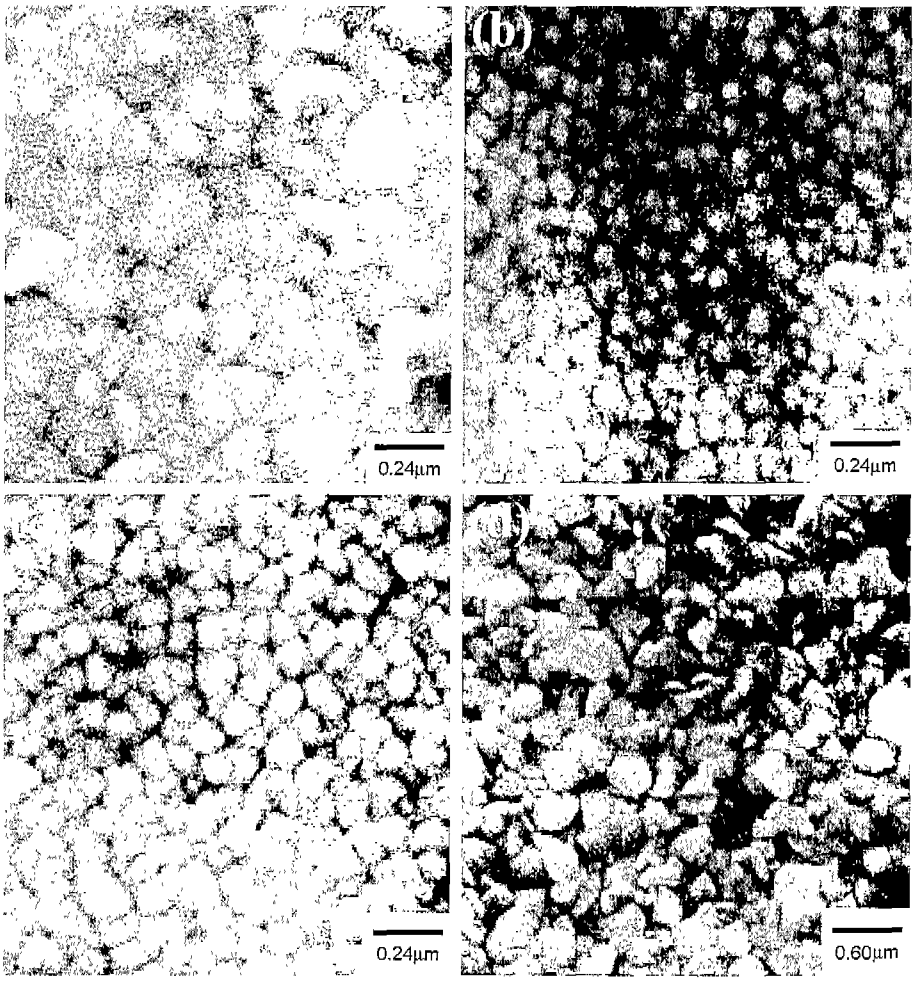

Fig. 5. SEM views of the ZnO films. The films were deposited at 250 W for 1 hour; the substrate temperature was R.T.; the R values were (a) 0.7%, (b) 2%, (c) 50%, and (d) 0%, respectively.

films were analyzed by scanning electron microscopy (SEM, Hitachi X-650) and atomic force microscopy (AFM, Topometrix, ACCUREX). The microstructural and crystallographic analysis of the films was performed by X-ray diffraction (XRD, Philips, PW3719) and transmission electron microscopy (TEM, Philips, CM200). The Rutherford backscattering spectroscopy (RBS) technique was used to determine the chemical composition of the films. In RBS, 2 MeV He^+ ions were used as incident particles and a backscatter angle of 170° was employed. Quantitative chemical analysis was carried out by computer simulation of the experimental RBS data with RUMP program.[9]

III. Results and Discussion

1. Thin film growth and microstructure

Fig. 2 shows the XRD spectra of the ZnO and AZO thin films deposited at substrate temperatures of 25~500°C. It is observed that {002} crystallographic planes of the films grown at 500°C tend to lie parallel to substrate surface. This indicates that the sputtered particles arriving at the substrate surface have enough energy to move around at 500°C, forming the closest packed planes.

The AFM images of the films are shown in Fig. 3. With the addition of Al, the average grain size decreased by a half and the surface roughness also decreased. This seems to be because the density of nucleation sites increased at initial state of film growth with the addition of Al. The nucleation sites can to be produced by the limited incorporation of Al into ZnO lattice.[10] Even though the target has about 2.0 at.% of Al, it is estimated that the concentration of Al in the films is about 1 at.%, based on the concentration of the charge carriers of the films; this will be discussed in the following section.

Fig. 4 shows how the intensity of the 002 peak in the XRD spectra changed with the oxygen fraction in the sputter gas. With increasing the oxygen fraction (R%) in the sputter gas from zero, the peak intensity increased, reaching its maximum at R=1.3%. At R>2.0%, the peak intensity decreased with increasing the R value. The grains of the films deposited at R=0% were considerably random-oriented (Fig. 5(d)). As the oxygen fraction in the sputter gas became near 2%, the grain size decreased and the film appeared to become denser (Fig. 5b, c); the growth rate of the films decreased and the packing density of the film increased.

The films prepared in pure Ar (R=0%) has oxygen deficiency of about 25%, as shown in Fig. 6. When the oxygen fraction in the sputer gas was 2%, the composition was Zn:O=1.05:1. On the other hand, when the oxygen fraction in the sputter gas was 30%, the composition was Zn:O=0.90:1. It was also found that the thickness of the films decreased with the addition of oxygen in the sputter gas.

The oxygen in the mixed Ar-O_2 sputter gas is thought to play a crucial role in reducing the deposition rate as well as the cation-to-anion ratio of the films. Such decrease is

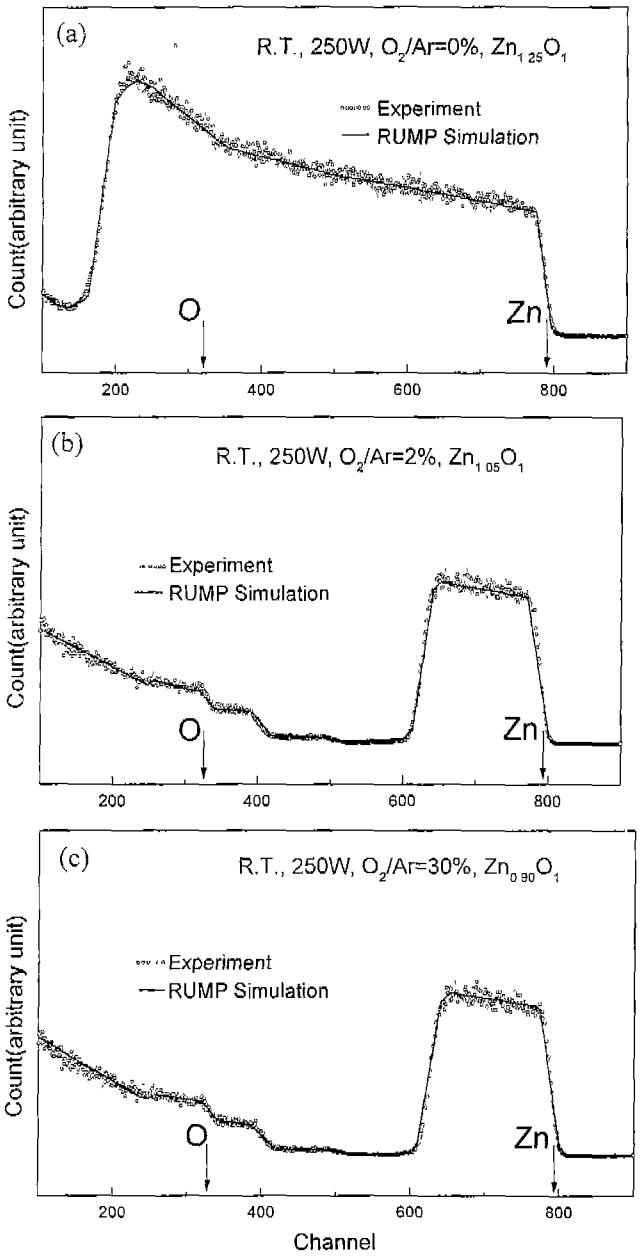

Fig. 6. RBS spectra of the ZnO films. The films were prepared at 250 W in various sputter gas; (a) R=0%, (b) R=2%, (c) R=30%. The substrate temperauter was R.T.

believed to occur by the chemisorption of excited oxygen on the surface of the target.[11,12] This, as a result, caused the film to exhibit the highest orientation preference, nearly stoichiometric composition, and good crystalline quality at R=1.3~2.0% in this experiment.

Fig. 7 shows SEM micrographs of the films deposited at sputter power of 100~250 W . The substrate temperature was kept at 500°C. Grain size of the films increased with sputter power. Microstructural changes with sputter power was investigated by XRD, and these are shown in Fig. 8. The film growth rate increased linearly with sputter power, but the FWHM decreased. The (002) peak was observed to

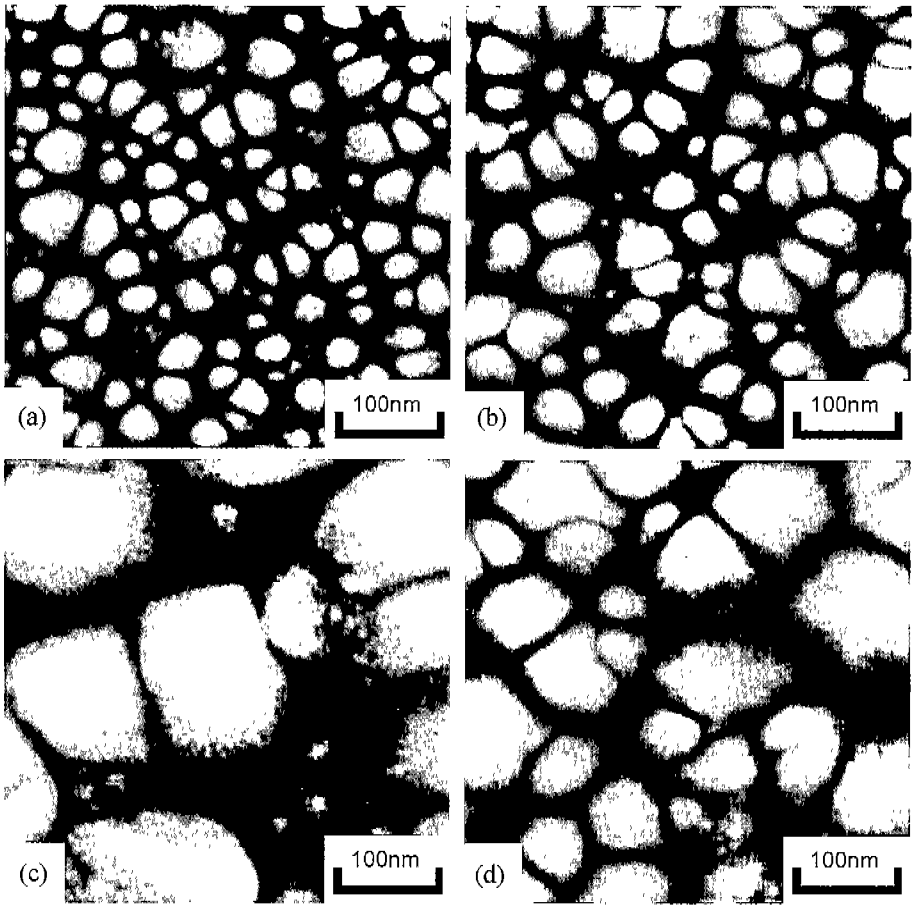

Fig. 7. SEM views of the AZO films. The films were prepared at various sputter power of (a) 100, (b) 150, (c) 200 and (d) 250 W, respectively. The substrate temperature was 500°C.

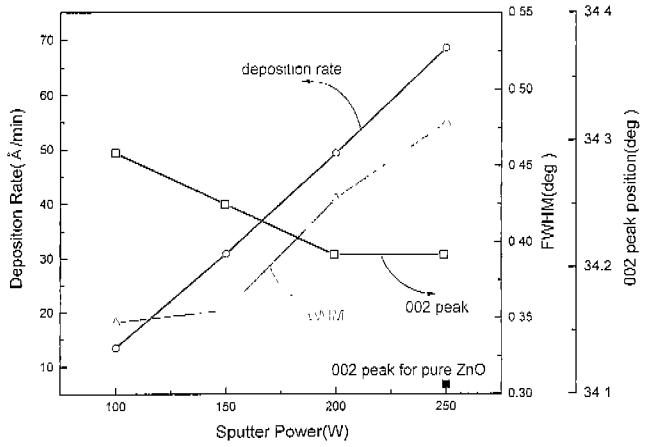

Fig. 8. Variation in the deposition rate, FWHM, and (002) peak position with sputter power. The films were deposited with various sputter power ranging from 100 to 250 W.

shift to low angle. These are regarded to occur because the crystalline quality and the substitution of Al at Zn sites decreased as the deposition rate increased.

2. Electrical features

The electrical resistivity of the ZnO and AZO films is shown in Fig. 9. The resistivity of the AZO films decreases remarkably as the deposition temperature increases. There is relatively large difference in resistivity at low substrate temperature depending on sputter power than at high substrate temperature; the resistivity of the films deposited at sputter power of 100 W was ~10^2 times higher than that of the films prepared at sputter power of 250 W; these films were prepared at 100°C. The microstructure and crystallinity of the films varied sensitively with the sputter power; the average grain size increases from ~30 to ~100 nm as sputter power raises from 100 to 250 W. Such a variation in microstructure and crystallinity with sputter power seem to affect the electrical mobility as well as carrier concentration in the films in a complicated way. In addition, all the AZO films prepared at 500°C exhibit semiconducting behavior (resistivity=10^{-1}~10^{-2} Wcm), and the variation in resistivity with sputter power is more less reversed from the case at 100°C.

Fig. 10 shows the TEM diffraction patterns obtained from the plane-view specimens of the AZO films deposited at 500°C (a) and 100°C (b), respectively. These films were prepared at sputter power of 250 W. AZO films prepared at 500°C exhibit good crystalline quality as well as highly preferred orientation with c-axis perpendicular to substrate sur-

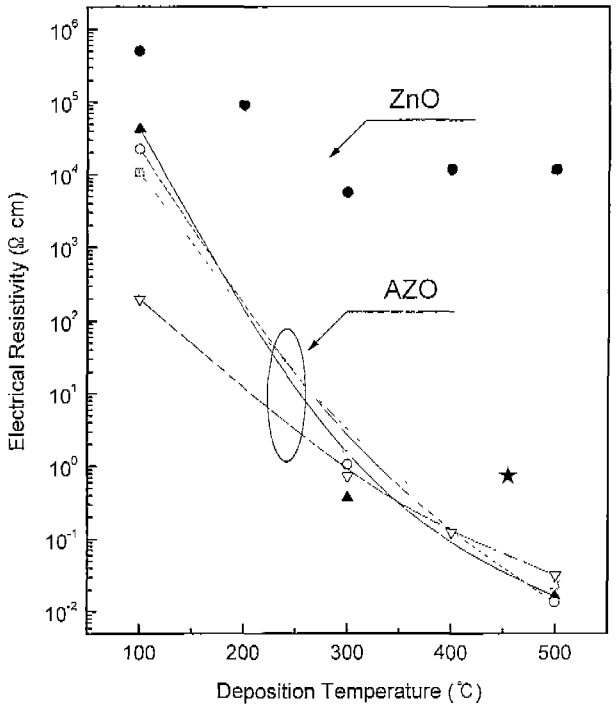

Fig. 9. Variation in the electrical resistivity of the ZnO and AZO films with deposition temperature. All the films were prepared at R=2%. The ZnO films were grown at 250 W. The AZO films were prepared at various sputter powers; the closed triangle, open circle, closed square, and open triangle in the plot indicate the variation of the resistivity of the AZO films which were prepared at 100, 150, 200, and 250 W, respectively. The asterisk indicates the electrical resistivity of the ZnO films, which were grown at 250 W and then annealed in reduced atmosphere of N_2:H_2=3:5 for 1 hr.

faces.

As a consequence, preferred orientation enlarges the mean free path of the charge carrier along the c-axis direction, while nearly continuous lattice planes frequently observed across the low-angle tilt grain boundaries reduce boundary scattering. These microstructural features increase the electron mobility of the films deposited at 500°C, compared with that of the films grown at temperatures lower than 500°C. As the substrate temperature increases, the resistivity of the AZO films declines by virtue of the microstructural features as well as higher crystallinity.

In contrast, the ZnO films have resistance of above 10^4 Ωcm, much higher than that of the resistivity of the films reduced in N_2-H_2 atmosphere, as shown in Fig. 9. It is possible to decrease the resistivity of the films by adding particular elements as well as post-deposition heat-treatment. For instance, Al is doped in this study and the relevant defect chemistry is expressed in eq. (2)

$$Al = Al^{\cdot}_{Zn} + e' \quad (2)$$

The relevant defect chemistry for the latter case is expressed in eq. (3).

$$O_O = 1/2O_2(g) + V^{\cdot}_O + e' \quad (3)$$

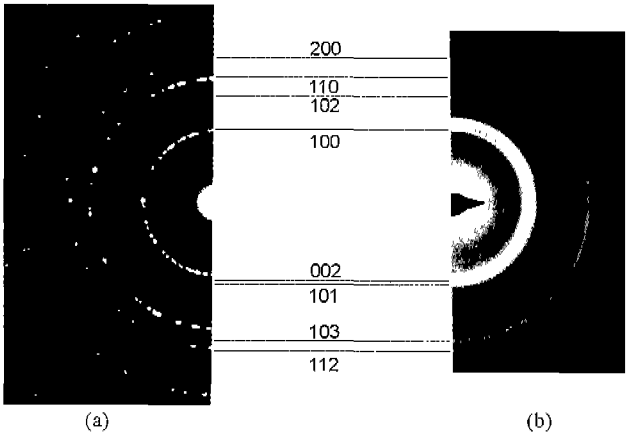

Fig. 10. TEM diffraction patterns of the AZO films. The films were deposited at (a) 500°C and (b) 100°C, respectively. The sputter power was 250 W, while the R value was 2%.

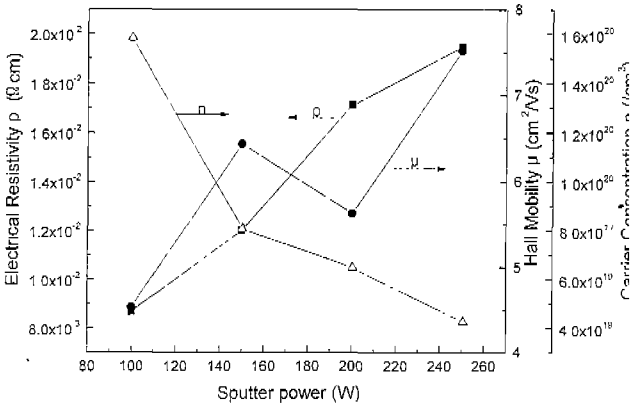

Fig. 11. Variation in the Hall mobility and carrier concentration of the AZO films with sputter power. The films were prepared in sputter gas of R=2% and at a substrate temperature of 500°C.

Each case, electrons are generated as charge carriers.

The resistivity, Hall mobility, and carrier concentration of the AZO films with sputter power are shown in Fig. 11. For the AZO films deposited at 500°C, the concentration of mobile electrons ranges from 4×10^{19} to 1.6×10^{20}/cm^3 depending on sputter power, and the mobilities are about a few cm^2/Vsec.

The mobile electrons in the AZO films is believed to be produced by the process described in the above reaction (2); so the concentration of Al substituting Zn ions in the lattice is about 1 at.%. Consequently, the crystallinity, grain size, Al-substitution, and the electrical features vary with sputter power; the films deposited at 250 W exhibit larger grains than the films grown at 100 W; but the former exhibits lower crystallinity that the latter. The carrier concentration as well as electrical conductivity of the films grown at 250 W is much lower than those of the films prepared at 100 W, mainly because the former has lower crystallinity and as a result lower Al-substitution, compared with the latter.

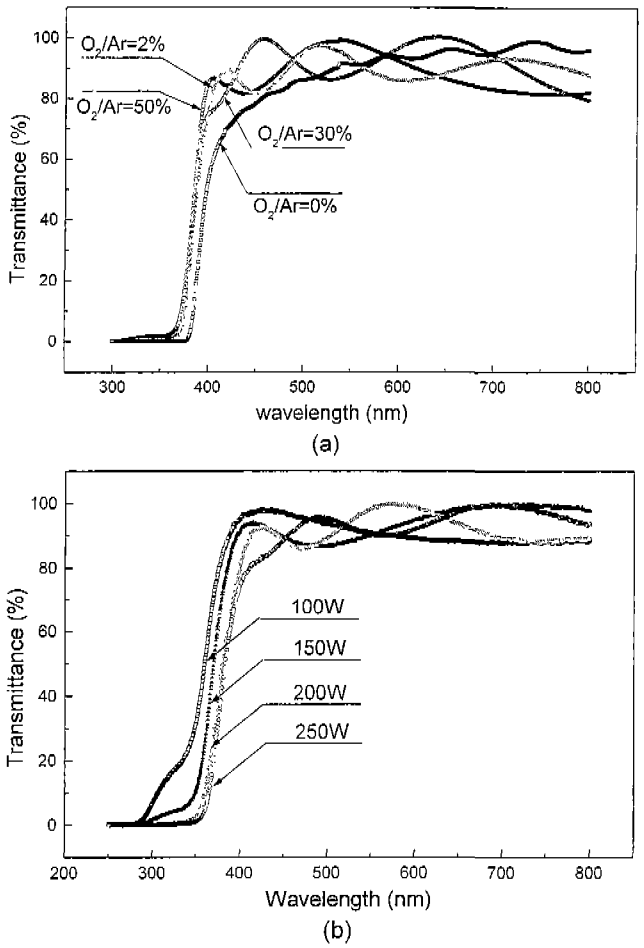

Fig. 12. UV-visible spectra of the films. (a) The ZnO films were deposited at 250 W and at a substrate temperature of R.T. for 1 hour in various sputter gas(R=0-50%). (b) The AZO films were prepared at various sputter power in pure Ar gas at 500.

3. Optical features

Fig. 12 shows the optical transmittance of the ZnO and AZO thin films. The ZnO films were prepared in sputter gas of R=0~50% at 25°C; the sputter power was 250 W. The AZO films were deposited in pure Ar gas at 500°C; the sputter power ranged from 100 to 250 W.

In Fig. 12(a), absorption edge is observed to shift to high frequency with increasing the R value. As the rf power increases, the absorption edge of the AZO films moves to longer wavelength region (Fig. 12(b)).

Variation of absorption coefficient with photon energy is shown in Fig. 13. The absorption coefficient of the films was calculated from the above transmittance spectra using the following relation

$$\frac{I}{I_0}(\text{transmit tan ce}) = c^{-at} \tag{4}$$

where I is the intensity of transmitted light, I_0 is the intensity of incident light, and t is the thickness of the film. In direct transition semiconductor(such GaAs, InSb and many

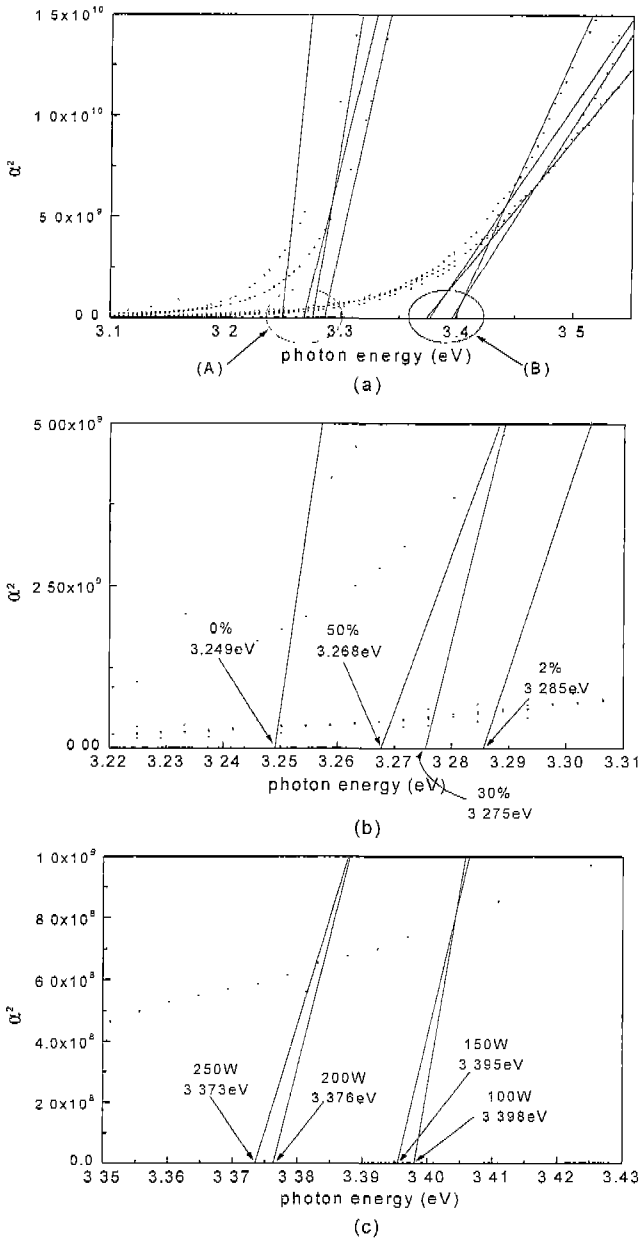

Fig. 13. Square of the absorption coefficient vs. photon energy (a) for the ZnO and AZO films. (b) and (c) are enlarged views of the energy region indicated with letters (A) and (B) in (a), respectively.

of III-V, II-VI compounds) with parabolic bands, the optical band gap (E_g) and the absorption coefficient could be described by the following relation.[13]

$$\alpha = A(h\nu - E_g)^{1/2} \tag{5}$$

where h is the Plank's constant, υ is the frequency of the incident photon, and A is a constant determined by the band property. The absorption edge of the films was obtained from the plot of α^2 vs hν.

In Fig. 13(a), the absorption edge of the ZnO films is about 3.25 eV(part(A)), while that of the AZO films is about 3.4

eV(part(A)).

Fig. 13(b) is an enlarged view of part (A) in Fig. 13(a). The absorption edge of the ZnO films changes with the R value. The film deposited at R=0% has the absorption edge of 3.25 eV, and the edge slightly increases to 3.29 eV when the R value is 2%.

Fig. 13(c) is an enlarged view of part (B) in Fig. 13(a). The absorption edge of the AZO films shifts to lower energy with increasing sputter power. As shown in Fig. 11, the electrical conductivity as well as carrier concentration of the AZO films change with sputter power. With increasing sputter power from 100 to 250 W, the concentration of charge carriers decreased from 1.6×10^{20} to $4\times10^{19}/cm^3$; this variation seems to be related with the crystallinity, as discussed previously. It is also regarded that the observed variation in absorption edge is associated with the Burstein-Moss shift.[14-16] The shift is caused by the variation in Fermi level in conduction band associated with the high concentration of charge carriers in the AZO films.

The kinetic energy of the sputtered atoms decreases monotonically as the pressure of the sputter gas increases, when the mass of the sputtered atom is greater than that of the sputter gas atoms.[17] But this is not the case, when the mass of sputtered atoms is lighter than that of the sputter gas atoms. The pressure of Ar sputter gas was kept constant at 10 mTorr in our experiment, and in this rather high sputter pressure the above results seems to be quite applicable. The difference in the kinetic energy of Al and Zn is large because of the selective decrement of the kinetic energy. So it is highly likely that high deposition rate at high sputter power caused deterioration in crystallinity and doping level, resulting in decrease in carrier concentration.

IV. Conclusion

ZnO and Al doped ZnO films were prepared by rf magnetron sputter technique. The films have a strong tendency that {002} planes lie parallel to substrate surface at 500. When the oxygen fraction in sputter gas was 2%, the ZnO films exhibited the composition of Zn:O=1.05:1. The films prepared at 250 W contain larger grains than the films grown at 100 W. However, high deposition rate seems to deteriorate the crystallinity as well as Al-substitution, resulting in lower concentration of mobile electrons. The Al-doped ZnO films which were deposited at 500°C show resistance of 1×10^{-2} Wcm; optical band gap of the films ranges from 3.25 to 3.40 eV. These electrical and optical features are related with microstructural as well as crystalline characteristics of the films.

References

1. Z. C. Jin, I. Hamberg and C. G. Granqvist, "Optical Properties of Sputter-Deposited ZnO:Al Thin Films," *J. Appl. Phys.*, **64**, 5117-5131 (1988).
2. H. Sato, T. Minami and S. Takata, "Highly Transparent and Conductive Group IV Impurity-doped ZnO Thin Films Prepared by RF Magnetron Sputtering," *J. Vac. Sci. Technol.*, **A11**, 2975-2979 (1993).
3. T. Minami, H. Nanto and S. Takata, "Highly Conductive and Transparent Aluminum Doped Zinc Oxide Thin Films Prepared by RF Magnetron Sputtering," *Jpn J. Appl. Phys.*, **23**, **5**, L280-282 (1984).
4. S. Matsushima, K. Abe, K. Kobayashi and G. Okada, "Oxygen-sensing Properties of Sputtered ZnO Film Deposited on Sapphire under Ultraviolet Illumination," *J. Mater. Sci. Lett.*, **11**, 389-391 (1992).
5. E. Ye. Gutman and I. A. Myasnikov, "The Kinetic Semiconductor Gas-sensor Conduction Model and Its Practical Use in Gas Analysis," *Sensors and Actuators*, **B13-14**, 687-691 (1993).
6. H. Nanto, H. Sokooshi and T. Usuda, "Small Sensor Using Aluminum-doped Zinc Oxide Thin Film Prepared by Sputtering Technique," *Sensors and Actuators*, **B10**, 79-83 (1993).
7. I. Sieber, N. Wanderka, I. Urban, I. Dorfel, E. Schierhorn, F. Fenske and W. Fuhs, "Electron Microscopic Characterization of Reactively Sputtered ZnO Films with Different Al-doping Levels," *Thin Solid Films*, **330**, 108-113 (1998).
8. Y. E. Lee, Y. J. Kim and H. J. Kim, "Thickness Dependence of Microstructural Evolution of ZnO Films Deposited by RF Magnetron Sputtering," *J. Mater. Res.*, **13**, 1260-1265 (1998).
9. L. R. Doolittle, Ph.D. Thesis, Cornell University (1987).
10. K. H. Kim, K. C. Park and D. Y. Ma, "Structural, Electrical and Optical Properties of Aluminum Doped Zinc Oxide Films Prepared by Radio Frequency Magnetron Sputtering," *J. Appl. Phys.*, **81**, 7764-7771 (1997).
11. N. Croitoru, A. Sedman and K. Yassin, "Some Physical Properties of ZnO Sputtered Films," *Thin Solid Films*, **150**, 291-301 (1987).
12. K. Tominaga, M. Kataoka and H. Manabe, T. Veda and I. Mori, "Transparent ZnO:Al Films Prepared by Co-sputtering of ZnO:Al with either a Zn or an Al Target," *Thin Solid Films*, **290-291**, 84-87 (1996).
13. J. I. Pankove, Optical process in semiconductor, Dover, New York (1975).
14. A. Sarkar, S. Ghosh and S. Chaudhuri and A. K. Pal, "Studies on Electron Transport Properties and the Burstein-moss Shift in Indium-doped ZnO Films," *Thin Solid Films.*, **204**, 255-264 (1991).
15. Z. C. Zin, I. Hamberg and C. G. Garnqvist, "Optical Properties of Sputter deposited ZnO:Al Thin Films," *J. Appl. Phys.*, **64**, 5117-512 (1988).
16. T. Minami, H. Nanto and S. Takata, "Optical Properties of Aluminum Doped Zinc Oxide Thin Films Prepared by RF Magnetron Sputtering," *Jpn. J. Appl. Phys.*, **24**(8), L605-608 (1985).
17. J. L. Vossen and W. Kern, Thin Film Processes, Academic Press, Inc., New York (1978).